Bioorganic & Medicinal Chemistry Letters 22 (2012) 2033–2042

Contents lists available at SciVerse ScienceDirect

Bioorganic & Medicinal Chemistry Letters

journal homepage: www.elsevier.com/locate/bmcl

The discovery of aminopyrazines as novel, potent $Na_v1.7$ antagonists: Hit-to-lead identification and SAR

Howard Bregman [a,*], Hanh Nho Nguyen [a], Elma Feric [b], Joseph Ligutti [d], Dong Liu [d], Jeff S. McDermott [b], Ben Wilenkin [b], Anruo Zou [d], Liyue Huang [c], Xingwen Li [c], Stefan I. McDonough [b], Erin F. DiMauro [a]

[a] Department of Chemistry Research and Discovery, Amgen Inc., 360 Binney St., Cambridge, MA 02142, USA
[b] Department of Neuroscience, Amgen Inc., 360 Binney St., Cambridge, MA 02142, USA
[c] Department of Pharmacokinetics and Drug Metabolism, 360 Binney St., Cambridge, MA 02142, USA
[d] Department of Neuroscience, Amgen Inc., One Amgen Center Drive, Thousand Oaks, CA 91320, USA

ARTICLE INFO

Article history:
Received 8 December 2011
Revised 6 January 2012
Accepted 9 January 2012
Available online 18 January 2012

Keywords:
$Na_v1.7$
Analgesia
Sodium channels
Aminopyrazine

ABSTRACT

Herein the discovery of a novel class of aminoheterocyclic $Na_v1.7$ antagonists is reported. Hit compound **1** was potent but suffered from poor pharmacokinetics and selectivity. The compact structure of **1** offered a modular synthetic strategy towards a broad structure–activity relationship analysis. This analysis led to the identification of aminopyrazine **41**, which had vastly improved hERG selectivity and pharmacokinetic properties.

The treatment of chronic pain represents a significant unmet medical need in society, providing an impetus for effort toward the identification of novel and efficacious medicines. Compelling human genetic data has implicated $Na_v1.7$ as a key mediator in nociception, sparking broad efforts aimed at $Na_v1.7$ antagonism across the scientific community.[1–3] One of the paramount challenges is the identification of chemical matter which possesses selectivity over physiologically important ion channels such as human Ether-a-go-go Related Gene (hERG) and subtype selectivity over similar channels within the Nav family, such as the cardiac channel $Na_v1.5$.

A high throughput screening campaign utilizing the IonWorks® Quattro automated electrophysiology platform[4,5] yielded amino-triazine (**1**). We utilized the IonWorks® Quattro (IWQ) and PatchXpress® (PX) planar patch-clamp automated electrophysiology platforms for screening and hit-to-lead assessments, respectively.[5] These assays enabled receptor–ligand interactions to be quantified directly, with a readout of functional inhibition, and allowed compound potency to be determined against defined gating states of sodium channels. The vast majority of sodium channel antagonists used clinically exert preferential inhibition of channel inactivated states, a property thought to confer functional selectivity for the sodium channels of hyperexcitable neurons. Accordingly, compound potency was assessed using the PX system on $hNa_v1.7$ with an average 20% contribution from inactivated channels.

Hit molecule (**1**) was a moderately potent, state-dependent $hNa_v1.7$ inhibitor ($hNa_v1.7$ manual IC_{50}-partially inactivated/closed = 0.3/2.9 μM) with low intrinsic clearance in human and rat liver microsomes (HLM, RLM intrinsic clearance = 25, 38 μL/min/mg) (Fig. 1). The structure of **1** was compact and amenable to rapid SAR evaluation. Although **1** exhibited low intrinsic clearance in liver microsomes, it suffered from poor solubility[6] and was rapidly metabolized in rat plasma resulting in extremely high clearance.[7] In addition, compound **1** lacked selectivity over the cardiac channels $hNa_v1.5$ and hERG. We embarked on SAR investigations with the goal to improve potency, selectivity and pharmacokinetic properties. For this effort, we routinely employed PX for assessment of potency on $hNa_v1.7$ and $hNa_v1.5$, dofetilide displacement for assessment of binding to hERG, and in vitro metabolic stability assays in liver microsomes and rat plasma to screen new molecules. The best new leads were further examined with additional electrophysiology (manual[8] on $hNa_v1.7$ and $hNa_v1.5$, and PX on hERG) and dosed in vivo to obtain rat PK data.[5]

The exceedingly high in vivo clearance (>10 L/h/kg) of **1** was found to be mediated in large part by plasma instability; thus our initial efforts were geared towards overcoming this liability. To understand the source of instability, compound **1** was analyzed

* Corresponding author.
E-mail address: hbregman@amgen.com (H. Bregman).

0960-894X/$ - see front matter © 2012 Elsevier Ltd. All rights reserved.
doi:10.1016/j.bmcl.2012.01.023

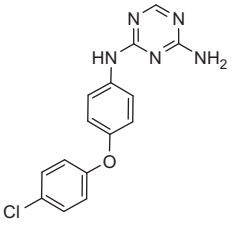

hNa$_v$1.7 PX IC$_{50}$ (μM)	2.2[a]
hNa$_v$1.7 Manual IC$_{50}$ (μM) 20% inactivated / closed	0.3 / [2.9][a]
hNa$_v$1.5 PX IC$_{50}$ (μM)	3.2[a]
hNa$_v$1.5 Manual IC$_{50}$ (μM) 20% inactivated / closed	0.2 / [> 10][a]
hERG dofetilide binding Ki derived , PX IC$_{50}$ (μM)	2.3 , 1.5
HLM , RLM intrinsic clearance (μL/min/mg)	25 , 38
Binding efficiency (kcal/NHA)	0.35[b]
Symyx solubility - SIF, PBS (pH 7.4), 0.01 N HCl (μg/mL)	7 , 1 , 6
clogP , PSA	4.6 , 86

[a]Electrophysiology IC$_{50}$ of partially inactivated channels is shown.[5] Where applicable, bracket indicates IC$_{50}$ against fully noninactivated channels determined with manual electrophysiology. Inhibitory activity represents an average of at least two determinations. [b]Binding efficiency = RT [log(hNav1.7 PX IC$_{50}$)]*(1x10^{-6})/(number of heavy atoms)

Figure 1. Profile of hit compound **1**.

after various incubation times in rat plasma by mass spectrometry.[7] After 3 h of incubation in fresh rat plasma near complete conversion to a single mono-N-oxidized product was observed. Towards improving plasma stability, the primary aniline group was methylated (**2**) or removed (**3**), leading to a substantial loss of potency in both cases (Table 1).

Alternatively, we looked towards modification of the triazine core as a means of modulating the electronics and nucleophilicity of the amine functionalities in hopes of reducing in vivo clearance while retaining potency (see Table 2). Pyrimidines **4** and **5** were prepared, each with one nitrogen removed from the core relative to **1** at a position proximal to the primary aniline. Compound **4** had improved potency relative to **1** (0.44 vs 2.2 μM) and substantially reduced rat IV clearance (CL = 2.0 L/h/kg), and pyrimidine **5** had greatly reduced potency (IC$_{50}$ >10 μM). Pyrimidine **6** was also prepared, which represents lead **1** with a core devoid of the most distal nitrogen relative to the primary aniline. Although the potency of **6** was retained relative to **1**, it was sevenfold less potent than pyrimidine **4**. Somewhat encouraged by the data for pyrimidines, we decided to explore pyridine cores. Pyridines **7** and **8** were greater than tenfold less potent than pyrimidine **4**. Pyridine **9** imparted modest Na$_v$1.5 selectivity (fourfold) but also was very active against hERG (IC$_{50}$ = 0.16 μM) and **10** suffered from high intrinsic clearance in liver microsomes.

Additional analogs were prepared in which the resulting core had two nitrogen atoms present, as in pyridazines **11** and **12** and pyrazine **13**. Pyridazine derivatives (**11** and **12**) suffered from a greater than tenfold reduction in potency relative to **4**. Pyrazine **13** possessed retained potency relative to **4**, and a fivefold selectivity over hERG, representing the first compound identified with any observed hERG selectivity. We also investigated replacement of two core carbon atoms with a sulfur atom. All three corresponding regioisomeric thiadiazoles (**14**–**16**) suffered from tenfold reduced potency relative to **4** and **13**. From our exploration of triazine core replacements we identified two new leads, pyrimidine **4**, which possessed improved potency (fivefold) and reduced rat IV clearance (2.0 L/h/kg) relative to hit **1**; and pyrazine **13** with improved potency (fourfold), and hERG selectivity (fivefold) as compared to **1**. Notably, both **4** and **13** were stable in rat plasma.

Initial follow-up SAR efforts on pyrimidine lead **4** were aimed towards augmenting hERG selectivity while retaining or improving potency and PK. We began with an evaluation of the linker region with the 4-amino pyrimidine core and *para*-chloro phenyl aryl tail group locked (Table 3). Replacement of the aniline NH with an oxygen (**17**) or the bottom ether with an amine (**18**) led to a loss of activity. Substitution of the bottom ether with a methyl amine (**19**) was better tolerated but still led to reduced potency relative to ether-linked lead **4**. Introduction of a methyl group at 3-position (**20**) or 2-position (**21**) yielded a >25-fold and fivefold decrease in activity, respectively. With no improved linker replacements identified we performed subsequent SAR assessments with the unsubstituted anilino-ether moiety locked as in lead **4**.

An initial study of positional substituent preference identified the *para* position as favorable. The chlorine substituent was moved from the *para* position (**4**) to the *meta* (**22**) and *ortho* (**23**) positions leading to a reduction in potency (fourfold and eightfold, respectively). Therefore, further aryl group SAR was performed at the

Table 1
Primary aniline substitution or removal

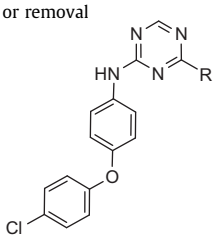

Compound	R	hNa$_v$1.7 PX IC$_{50}$[a] (μM)
1	NH_2	2.2
2	$NHCH_3$	>10
3	H	>10

[a] Electrophysiology IC$_{50}$ of partially inactivated channels is shown. Inhibitory activity represents an average of at least two determinations.[5]

Table 2
SAR of core modifications of **1**

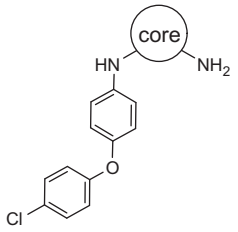

Compound	core	hNa$_v$1.7 PX IC$_{50}$[a] (μM)	hNa$_v$1.5 PX IC$_{50}$[a] (μM)	hERG K_i-derived (μM)	HLM CL$_{int}$ (μl/min/mg)	RLM CL$_{int}$ (μl/min/mg)	Rat plasma $t_{1/2}$ (min)	Rat IV CL (L/(h kg))[b]
1	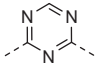	2.2	3.2	2.3	25	38	<30	>10
4	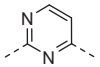	0.44	0.50	0.43	104	91	>500	2.0
5	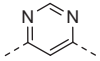	13.5	–	–	<14	32	–	–
6	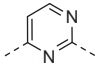	3.1	–	0.32	206	41	–	–
7	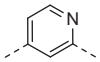	6.1	–	–	18	127	–	–
8	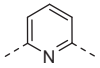	8.8	–	–	100	238	–	–
9	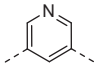	2.9	11.8	0.16	36	88	–	–
10	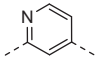	2.0	1.4	0.05	14	>399	–	–
11	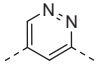	7.3	–	–	20	>399	–	–
12	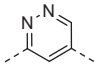	5.5	–	–	<14	>399	–	–
13	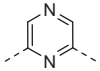	0.62	0.72	2.9	183	151	>500	8.2
14	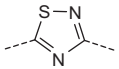	5.7	–	–	<14	<14	–	–
15	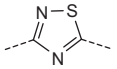	5.3	–	–	16	37	–	–
16	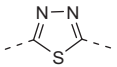	11.3	–	–	<14	<14	–	–

[a] Electrophysiology IC$_{50}$ of partially inactivated channels is shown. Inhibitory activity represents an average of at least two determinations.[5]
[b] Male Sprague-Dawley rats were dosed intravenously at 0.5 mg/kg in 0.5 mL/kg of 100% DMSO.

Table 3
Linker region SAR

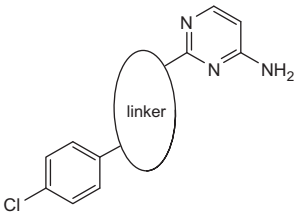

Compound	Linker	hNa$_v$1.7 PX IC$_{50}$[a] (μM)	hNa$_v$1.5 PX IC$_{50}$[a] (μM)	hERG K_i-derived (μM)	HLM CL$_{int}$ (μl/min/mg)	RLM CL$_{int}$ (μl/min/mg)
4	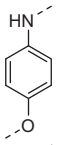	0.44	0.50	0.43	104	91
17	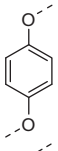	9.8	–	–	30	72
18	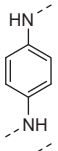	5.9	–	–	<14	28
19	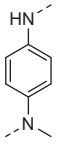	1.8	3.7	0.8	41	>399
20	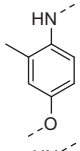	11.1	–	–	89	>399
21	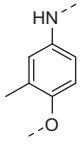	2.3	2.27	–	58	167

[a] Electrophysiology IC$_{50}$ of partially inactivated channels is shown. Inhibitory activity represents an average of at least two determinations.[5]

para position (Table 4). Replacement of the *para*-chloro substituent with fluorine (**24**) did not offer improvements in potency, selectivity, or intrinsic clearance. Methyl (**25**) and cyclopropyl (**26**) derivatives yielded a modest reduction in potency (~threefold) with a more profound drop observed for the larger phenyl derivative (**27**). Substitution with both electron withdrawing and electron donating polar substituents was studied. Electron withdrawing substitution, such as cyano (**28**), methyl sulfone (**29**), carboxamido (**30**), reduced Na$_v$1.7 potency. Pyridine analog (**31**) suffered a loss in potency. Bulky hydrophobic electron withdrawing groups such as trifluoromethyl (**33**) and trifluoromethoxy (**34**) led to slight reductions in potency (threefold and twofold, respectively), but improved microsomal stability. The electron donating dimethylamino (**32**) substitution was not tolerated. Our SAR evaluation of the tail aryl group with the pyrimidine core provided no improvement in potency or selectivity, but an understanding that retained potency and improved microsomal stability can be realized with the introduction of hydrophobic electron withdrawing groups at the *para* position.

We then embarked on a follow up effort to pyrazine lead **13**, which had selectivity over hERG, with the goal of improving upon its PK properties while retaining or improving potency and selectivity. Using lessons learned from the pyrimidine series work, we evaluated the effect of *para* substitution of the tail aryl ring, concentrating on substitution which had offered modest potencies and microsomal stabilities in the pyrimidine series (Table 5). Removal of the *para* substituent provided phenyl analog (**35**), which had retained potency and improved selectivity, along with low intrinsic clearance in HLM but high in RLM. Replacement of the chlorine with fluorine (**36**) provided retention or modest improvements in potency, selectivity and intrinsic clearance in HLM. *para* Substitution with a methyl group (**37**) did not offer any improvements, whereas cyclopropyl derivative (**38**) had improved hERG selectivity and microsomal stability but two-fold reduced potency. Compound (**39**) substituted with a small electron withdrawing cyano group suffered a drop in potency. Bulky hydrophobic electron withdrawing groups were evaluated as well. The trifluoromethyl derivative (**40**) yielded

Table 4
Amino-pyrimidine tail aryl SAR

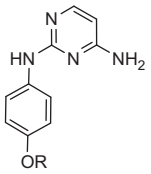

Compound	R	hNa$_v$1.7 PX IC$_{50}$[a] (μM)	hNa$_v$1.5 PX IC$_{50}$[a] (μM)	hERG K_i-derived (μM)	HLM CL$_{int}$ (μl/min/mg)	RLM CL$_{int}$ (μl/min/mg)
4	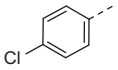	0.44	0.50	0.43	104	91
22		3.2	1.7	—	44	250
23		1.8	0.36	1.4	93	>399
24	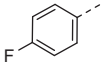	1.2	0.78	1.9	177	193
25		1.6	0.59	1.1	>399	161
26	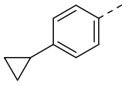	1.5	2.0	0.5	19	61
27	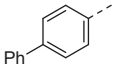	>30	—	—	—	—
28	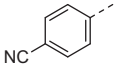	2.0	1.2	1.2	71	48
29	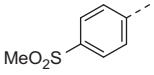	>30	—	—	22	<14
30	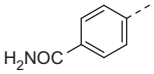	>30	—	—	—	—
31		25.7	—	—	<14	<14
32	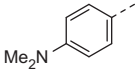	10.8	—	—	75	190
33	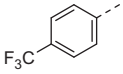	1.3	<1.0	0.9	24	23
34	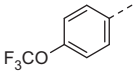	0.9	0.24	0.1	27	17

[a] Electrophysiology IC$_{50}$ of partially inactivated channels is shown. Inhibitory activity represents an average of at least two determinations.[5]

retained potency and hERG selectivity (tenfold) with reduced intrinsic clearance relative to the chloro lead (**13**). Even greater overall improvements were realized with trifluoromethoxy derivative (**41**) which was potent on Na$_v$1.7 (0.24 μM), selective over hERG and exhibited low intrinsic clearance in both HLM and RLM (27, 36 μl/min/mg, respectively) and better solubility in SIF (109 vs 7 μg/mL for **1**) (Fig. 2).

Compound **41** was further assessed in rat PK studies. Gratifyingly, the good intrinsic stability in liver microsomes and rat plasma translated to moderate rat IV clearance (0.93 L/h kg), and reasonable oral exposure (AUC$_{inf}$ (μM * h), C_{max} (μM) = 0.76, 0.22). Relative to hit compound **1**, structure **41** had two structural changes. Replacement of the triazine core with a pyrazine yielded (**13**), which had improved rat clearance and selectivity (see Table 2). By further replacing the *para*-Cl substituent with an OCF$_3$ group (**41**), significant improvements in microsomal stability were realized, which translated to moderate rat IV clearance, and improved selectivity over hERG (35-fold) and Na$_v$1.5 (fivefold (PX); twofold (manual)). Beyond the encouraging properties of lead **41**, the pyrazine series overall represents a promising starting point towards the development of selective and orally bioavailable Na$_v$1.7 antagonists. The general trend for selectivity over Na$_v$1.5 and hERG is clear upon visualization of the analogs described herein binned by core type (Fig. 3). The pyrazine analogs generally offer a better selectivity profile than pyrimidine analogs or other structures described. This selectivity enhancement, in concert with favorable rat pharmacokinetics, mark this series as a favorable starting point for future efforts.

Chlorotriazine **43** was obtained via S$_N$Ar of aniline **42** with 2,4-dichlorotriazine under basic conditions and was subsequently

Table 5
Amino-pyrazine tail aryl SAR

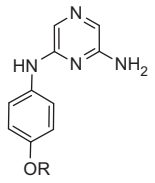

Compound	R	$Na_v1.7$ PX IC_{50}[a] (μM)	$Na_v1.5$ PX IC_{50}[a] (μM)	hERG K_i-derived (μM) or % in h @30 μM	HLM CL_{int} (μl/min/mg)	RLM CL_{int} (μl/min/mg)
13	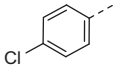	0.62	0.72	2.9	183	151
35		0.5	1.8	25%	<14	172
36	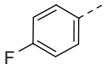	0.44	0.47	1.1	71	222
37	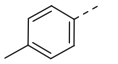	0.88	0.41	2.0	>399	129
38	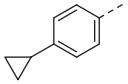	1.3	3.0	48%	33	70
39	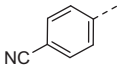	3.9	–	–	142	216
40	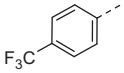	0.26	0.46	2.8	40	99
41	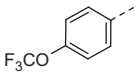	0.24	1.26	33%	27	36

[a] Electrophysiology IC_{50} of partially inactivated channels is shown. Inhibitory activity represents an average of at least two determinations.[5]

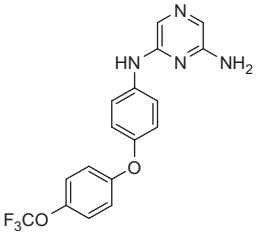

$hNa_v1.7$ PX IC_{50} (μM)	0.24
$hNa_v1.7$ Manual IC_{50} (μM) 20% inactivated / closed	0.80 / [>3][a]
$hNa_v1.5$ PX IC_{50} (μM)	1.3[a]
$hNa_v1.5$ Manual IC_{50} (μM) 20% inactivated / closed	1.5 / [10][a]
hERG dofetilide binding Ki derived , PX IC_{50} (μM)	77.3% inh. @ 30 μM , 8.5
HLM , RLM intrinsic clearance (μL/min/mg)	27 , 36
Rat IV CL (L/h-kg) , Vss (L/kg) , $t_{1/2}$ (h)	0.93 , 2.1 , 1.9[b]
Rat PO PK (%F , AUC_{inf} (μM * hr) , C_{max} (μM) , $t_{1/2}$ (h))	13 , 0.76 , 0.22 , 2.47[c]
Rat plasma protein binding (% bound)	99.9
CYP 3A4, 2D6 inh. IC_{50} (μM)	> 27
Binding efficiency (kcal/NHA)	0.35
Symyx solubility – SIF , PBS (pH 7.4) , 0.01 N HCl (μg/mL)	109 , 1 , 7
clogP , PSA	5.6 , 82

[a]Electrophysiology IC_{50} of partially inactivated channels is shown. Where applicable, bracket indicates IC_{50} against fully noninactivated channels determined with manual electrophysiology. Inhibitory activity represents an average of at least two determinations. [b]Male Sprague-Dawley rats were dosed intravenously at 0.5 mg/kg in 0.5 mL/kg of 100% DMSO. [c]Male Sprague-Dawley rats were dosed orally at 2.0 mpk in 10 mL/kg of vehicle (30% hydroxypropyl-β-cyclodextrin, pH 2.2 adjusted with methanesulfonic acid).

Figure 2. Profile of lead **41**.

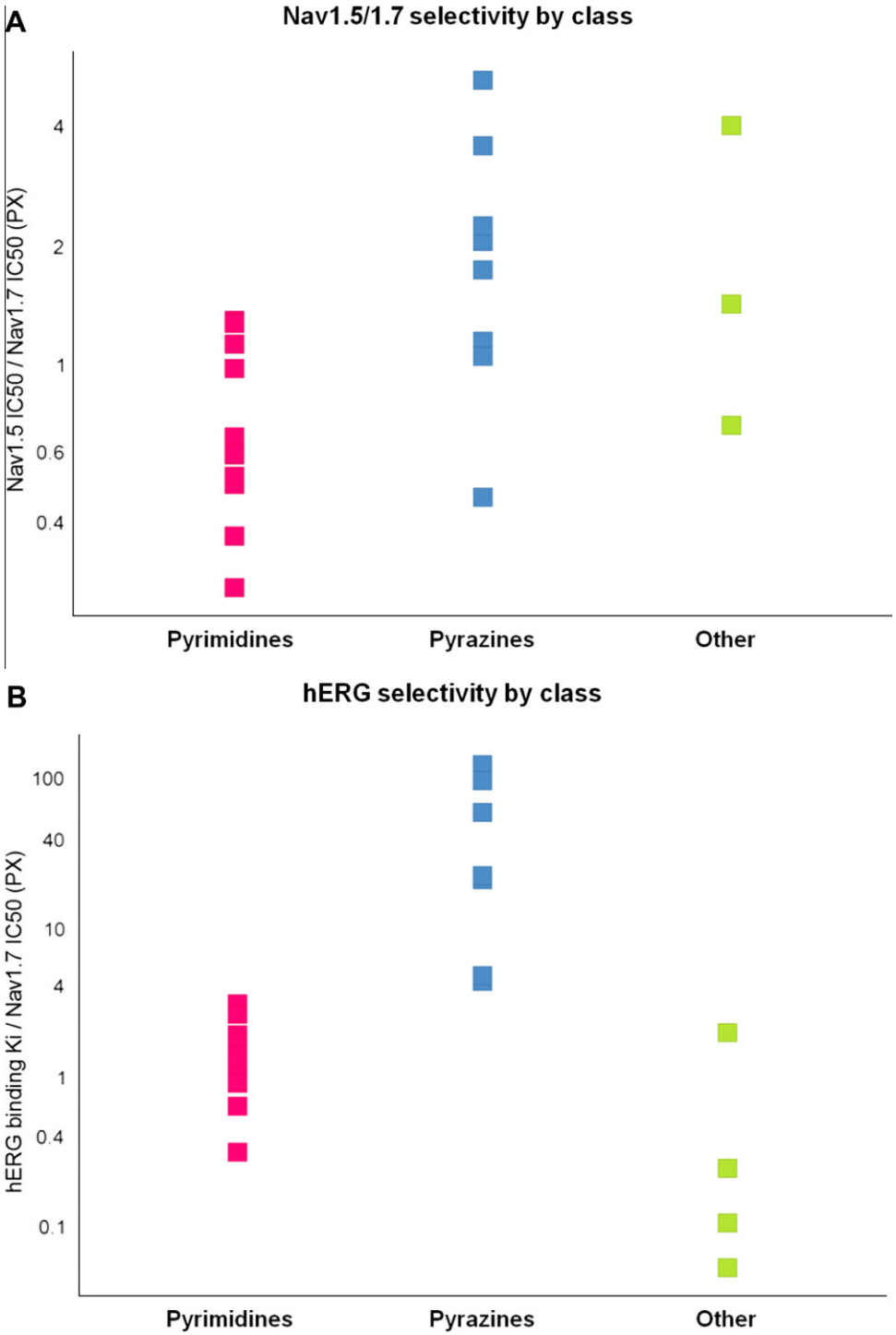

Figure 3. (A) Visualization of $Na_v1.5/1.7$ selectivity (log scale) binned by structural class. (B) Visualization of hERG/$Na_v1.7$ selectivity (log scale) binned by structural class.

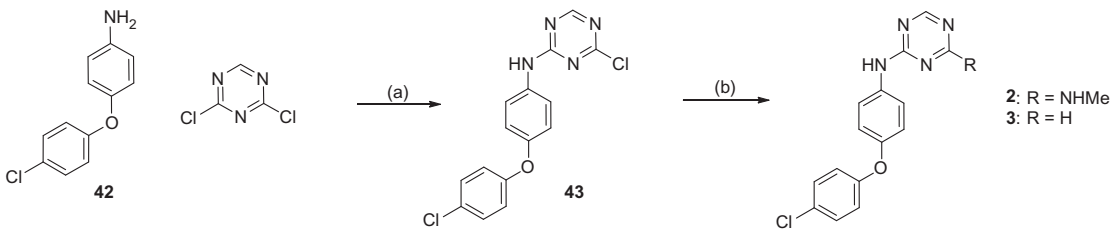

Scheme 1. Synthesis of RHS modified derivatives **2**–**3**. Reagents and conditions: (a) DIEA, DMF, 0 °C; (b) for **2**: $MeNH_2$, DMF, 0 °C to rt, 11% (2 steps); for **3**: Pd/C, H_2, MeOH, 21% (2 steps).

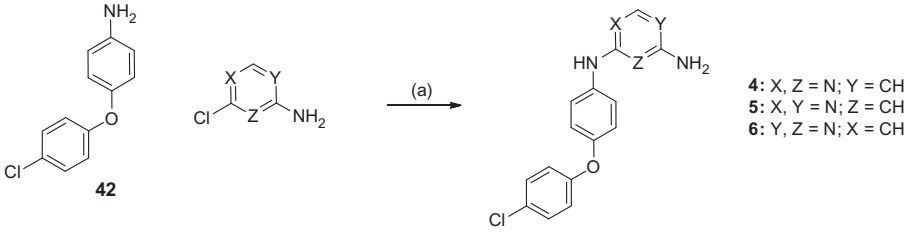

Scheme 2. Synthesis of core modified pyrimidine analogs **4**–**6**. Reagents and conditions: (a) HCl, H_2O, 100 °C, yield of **4**, **5**, **6**: 39%, 17%, 19%.

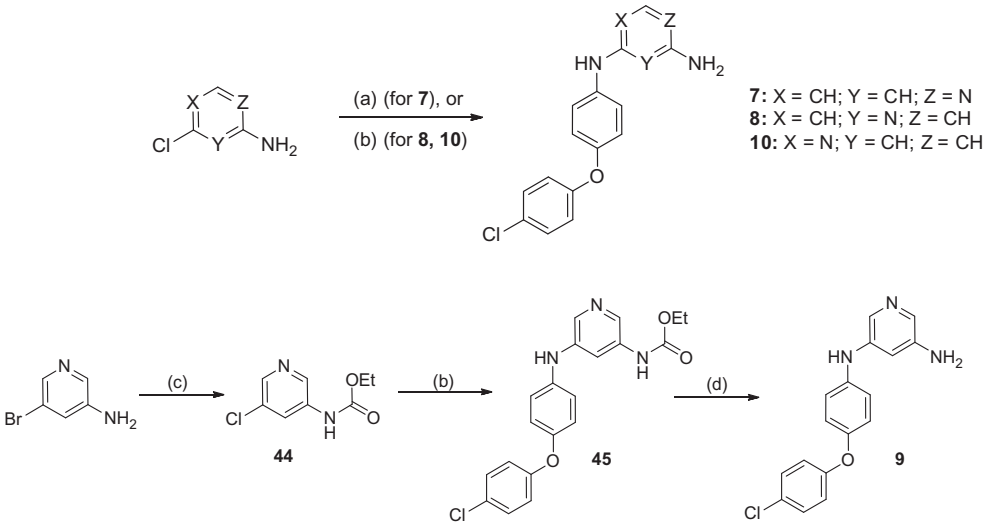

Scheme 3. Synthesis of core modified pyridine analogs **7**–**10**. Reagents and conditions: (a) Compound **42**, HCl, MeOH:H_2O (1:1), 100 °C, 30%; (b) **42**, $Pd_2(dba)_3$, BINAP, Cs_2CO_3, DMA, 120 °C, **8**, **10**: 23%, 12%; (c) ethyl chloroformate, pyridine, DCM; (d) KOH, EtOH, 70 °C, 11% (3 steps).

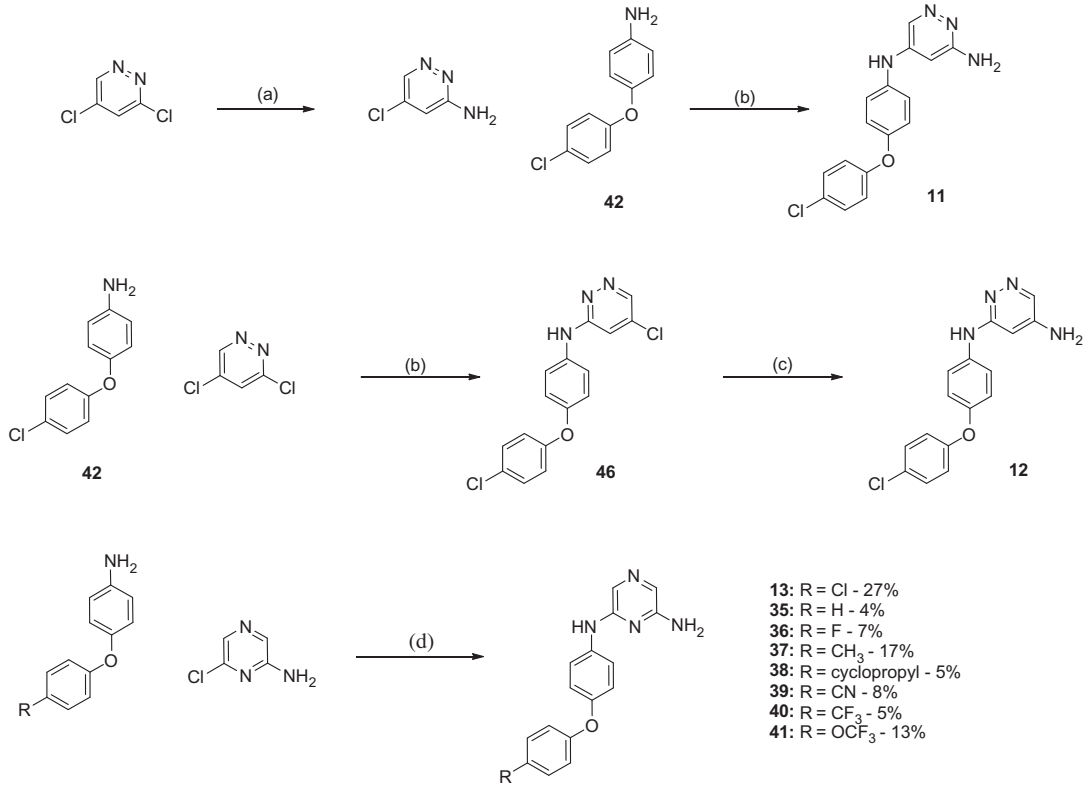

Scheme 4. Synthesis of core modified pyridazine analogs **11**,**12**, pyrazine analogs **13**, **35**–**41**. Reagents and conditions: (a) NH_3 (l), steel bomb, rt, 56%; (b) HCl, MeOH, 85 °C **11**, **46**: 3%, 35%; (c) NH_3 (l), steel bomb, 160 °C, 9%; (d) $Pd(OAc)_2$, BINAP, KO^{t}Bu, toluene, 120 °C, yields in scheme.

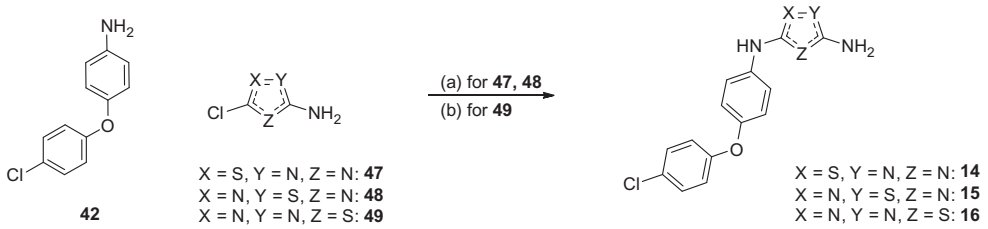

Scheme 5. Synthesis of core modified thiadiazole analogs **14**–**16**. Reagents and conditions: (a) HCl, MeOH, 100 °C, **14**, **15**: 25%, 26%; (b) Et_3N, THF, 80 °C, 33%.

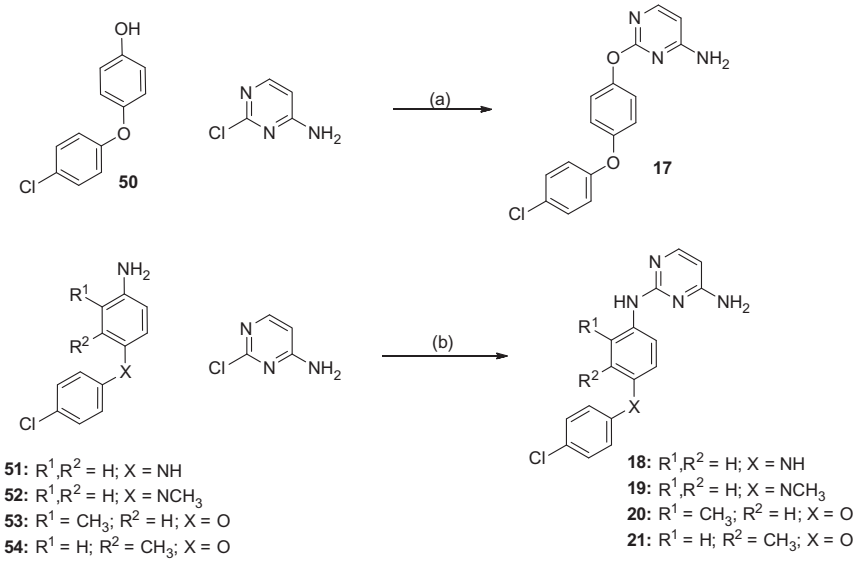

Scheme 6. Synthesis of linker modified pyrimidine analogs **17**–**21**. Reagents and conditions: (a) NaH, DMF, 100 °C, 15%; (b) HCl, MeOH, 100 °C, **18**, **19**, **20**, **21**: 40%, 23%, 36%, 22%.

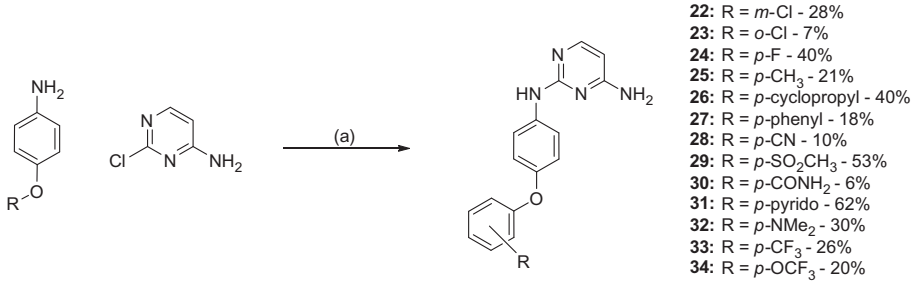

Scheme 7. Synthesis of tail-modified aryl ether pyrimidine analogs **22**–**34**. Reagents and conditions: (a) HCl, MeOH, 100–140 °C (thermal or microwave).

exposed to methyl amine in DMF providing **2** or reduced to afford **3** (Scheme 1).

Pyrimidines **4**–**6** were obtained via S_NAr of the appropriate chloro-amino pyrimidine precursor with aniline **42** under acidic conditions[9] (Scheme 2).

The 2-amino-4-anilino pyridine analog **7** was obtained via S_NAr with **42** under acidic conditions at elevated temperatures. The 2-amino-6-anilino and 4-amino-2-anilino pyridines (**8**, **10**) were synthesized from their respective chloro-amino pyridine precursors by Buchwald–Hartwig reactions. The 3-amino-5-anilino pyridine analog (**9**) was obtained through a three-step sequence: the protection of commercially available 5-bromo-3-amino pyridine as an ethyl carbamate (**44**); subsequent Buchwald–Hartwig amination (**45**) and hydrolytic deprotection yielded pyridine **9**[10] (Scheme 3).

The preparation of pyridazine analogs **11**, **12** proceeded via two-step protocols. Amination of commercially available 3,5-dichloropyridazine with ammonia at room temperature provided 5-chloropyridazin-3-amine. Subsequent S_NAr with aniline **42** under acidic conditions afforded **11**. Reversal of this sequence, but with amination of 4-chloropyridazine **46** at elevated temperatures (160 °C) afforded **12**. Pyrazine analogs **13**, **35**–**41** were prepared by Buchwald–Hartwig amination (Scheme 4).

The synthesis of 1,2,4-thiadiazole analogs **14**, **15** was accomplished via S_NAr reactions with aniline **42** under acidic conditions via their respective amino-chloro-thiadiazole precursors (**47**, **48**). The 1,3,4-thiadiazole analog (**16**) was obtained utilizing basic S_NAr conditions with aniline **42** (Scheme 5).

The synthesis of bis-ether analog **17** was accomplished utilizing an S_NAr reaction of 2-chloro-6-aminopyrimidine with the anion of

phenol **50**. Pyrimidines **18**–**21** were obtained via S_NAr under acidic conditions with anilines **51**–**54** (Scheme 6).

Pyrimidine analogs with modification of the tail aryl (**22**–**34**) were obtained with S_NAr of 2-chloro-6-aminopyrimidine with the appropriate aniline (Scheme 7).

Acknowledgement

The authors would like to thank Ramin Vismeh for plasma stability studies.

References and notes

1. Cummins, T. R.; Sheets, P. L.; Waxman, S. G. *Pain* **2007**, *131*, 243.
2. England, S.; Rawson, D. *Future Med. Chem.* **2010**, *2*, 775.
3. Zuliani, V.; Patel, M. K.; Fantini, M.; Rivara, M. *Curr. Top. Med. Chem.* **2009**, *9*, 396.
4. Bregman, H.; Berry, L.; Buchanan, J. L.; Chen, A.; Du, B.; Feric, E.; Hierl, M.; Huang, L.; Immke, D.; Janosky, B.; Johnson, D.; Li, X.; Ligutti, J.; Liu, D.; Malmberg, A.; Matson, D.; McDermott, J.; Miu, P.; Nguyen, H. N.; Patel, V. F.; Waldon, D.; Wilenkin, B.; Zheng, X. M.; Zou, A.; McDonough, S. I.; DiMauro, E. F. *J. Med. Chem.* **2011**, *54*, 4427.
5. The electrophysiology protocols for IonWorks Quattro® (IWQ), PatchXpress® (PX) and manual patch-clamp are described in this paper. IWQ protocol: $hNa_v1.7$ or $hNa_v1.5$-expressing HEK 293 cells (no exogenous beta-subunit was co-expressed) were patched in PPC mode (population patch clamp), and currents were measured in response to a train of depolarizations that induced successively greater inactivation. Dose–response curves were built from an ensemble of wells that were exposed to different single concentrations. PX protocol: $hNa_v1.7$ or $hNa_v1.5$-expressing HEK 293 cells (no exogenous beta-subunit was co-expressed) were voltage clamped at a membrane potential that produced average 20% fractional inactivation. Voltage was set, and reset as needed, to produce 20% inactivation, since state-dependent pharmacology is determined not by the absolute voltage but by fractional channel inactivation, and the voltage dependence of inactivation varies among cells and can vary with time when recorded from a single cell. Currents were corrected for rundown offline with DataXpress software, and dose–response curves were built from an ensemble of single-concentration tests on many cells. For experimental details of manual electrophysiology, see Bregman, H. et al. (Ref. 4.)
6. Tan, H.; Semin, D.; Wacker, M.; Cheetham, J. *JALA* **2005**, *10*, 364.
7. The plasma concentration of **1** was below the detection limit after 15 min following a single bolus intravenous administration at 0.5 mg/kg. Fresh rat plasma was incubated with (**1**) (dissolved in DMSO, final concentration in plasma was 10 μM) at 37 °C. 200 μL aliquots at 30 min, 1 and 2 h were pipetted out and mixed with 400 μL acetonitrile to precipitate proteins. Samples were centrifuged and supernatants were analyzed directly using LC/MS/MS. Analysis was performed using a dC18 column (Atlantis, 1 × 15 mm × 5 μm) coupled to a Thermo Scientific LTQ-Orbitrap XL mass spectrometer (Bremen, Germany) using a 50 min (5–95% acetonitrile with 0.1% formic acid) gradient in ESI positive mode. Identification of hydroxylated metabolite was based on exact mass measurement of protonated molecular ion (<1 ppm accuracy) and comparing MS/MS fragments to those of parent compound. The typical limit of detection is 0.5 ng/ml.
8. Manual electrophysiology verifies the PX value, controls for kinetic information and used to test compound potency on non-inactivated (closed) channels.
9. Rahman, A. A.; Daoud, M. K.; Dukat, M.; Herrick-Davis, K.; Purohit, A.; Teitler, M.; do Amaral, A. T.; Malvezzi, A.; Glennon, R. A. *Bioorg. Med. Chem. Lett.* **2003**, *13*, 1119.
10. Hasegawa, M.; Nishigaki, N.; Washio, Y.; Kano, K.; Harris, P. A.; Sato, H.; Mori, I.; West, R. I.; Shibahara, M.; Toyoda, H.; Wang, L.; Nolte, R. T.; Veal, J. M.; Cheung, M. *J. Med. Chem.* **2007**, *50*, 4453.